DUJASE Vol. 3(2) 135-142, 2016 (January)

Development of a ray tracing model to design an optical Asymmetric Compound Parabolic Concentrator (ACPC) for solar air heating collector using Matlab

S. M. Nasif Shams[1], MickMcKeever[2], Sarah McCormack[3] and Brian Norton[4]

[1] *Institute of Energy, Dhaka University, Dhaka, Bangladesh*

E-mail: nasifshams@gmail.com

[2]*Dublin Energy Lab, School of Electrical and Electronic Engineering, Dublin Institute of Technology, Ireland*

[3]*Dublin Energy Lab, Department of Civil, Structural and Environmental Engineering, Trinity College, Ireland*

[4]*Dublin Energy Lab, Dublin Institute of Technology, Dublin, Ireland*

Received on 12.05.2015. Accepted for publication on 14.06.2015.

ABSTRACT

This paper presents a ray tracing model to design an optical Asymmetric Compound Parabolic Concentrator (ACPC) concentrator using Matlab. The concentratorwas integrated with a Transpired Air Heating (TAH) system to develop Concentrating Transpired Air Heating (CTAH) collector. An asymmetric compound parabolic concentrator was applied to increase the intensity of solar radiation incident on the perforated absorber. This research simulates the optical performance of the concentrator using ray tracing technique and validates the model using laser test method. Matlab Software was used as the simulation tool. The maximum optical efficiency of the CTAH was 79.5% for 50 mm tertiary height, 88% transmittance of the glazing and 95% reflectance of the concentrator reflector for beam radiation. The acceptance angle of the CTAH varied between 100% at 27^o incident angle and 92.7% at incident angle 89^o which provides effective annual concentration for 7-8 hours. The optical efficiency within 27^o to 89^{o}incident angles varies between 79.5% and 72%.The sensitivity test was carried out for different properties of the concentrator and geometry of the reflector surface. The effect of the reflector material property and geometry was investigated in this research.

Keywords: Transpired Air Heating (CTAH), Air Heating, Concentrator.

1. Introduction

This research focuses on the design and experimental performance analysis of a stationary novel air heating system which is the integration of a Transpired Air-heating Collector (TAC) and an Asymmetric Compound Parabolic Concentrator (ACPC). The usefulness of the CPC for solar energy collection was noted by numerous researchers [1-8]. Air gain heat as it flows through the concentrated radiation below perforated absorber. Ray tracing technique was used commonly to determine the optical performance of concentrating solar energy systems in numerous research works [2-3, 9-10]. The front upper and lower surface of the optical CTAH geometry is highly asymmetric. However, the shape is symmetric in the longitudinal direction. A 2D ray tracing model was necessary to conduct optical analysis. A cross section of the geometrical CTAH was used as the boundary surface of the optical model where incident radiation intersects.

2. Geometric Design of the concentrator

CTAH is a combination of perforated absorber and Compound Parabolic Concentrator (CPC). CPC was designed for 20^o half acceptance angle and 100 mm absorber using Eq. (1).

$$y = \frac{x^2}{2b\left(1+\sin\theta_a\right)} \quad (1)$$

Where, b = absorber width, θ_a= half acceptance angle.

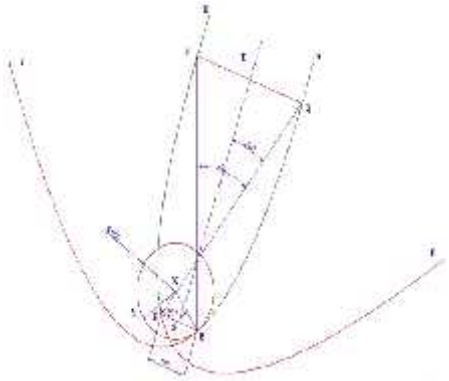

Fig. 1: Design of CTAH

The reflector design process has been detailed using Fig. 1, Fig. 2, and Fig. 3. Two parabolas of identical geometry were produced as ABC and DEF. B is focus of DEF and E is focus of parabola ABC. BE is the absorber of 100 mm width DEBA becomes an ideal CPC with an acceptance angle 40^o and TS is the centre axis of the CPC.

Fig. 2: Design of CTAH

Any radiation on the aperture PQ, within the acceptance angle will be received by the absorber BE. A circle is introduced to the point B and the left part of the CPC is transferred to the centre of the circle. Aperture is determined when the tangent of DE and BC is parallel to the CPC centre axis ST. In practice, CPC is generally truncated to reduce in height by 50 % in order to reduce its cost [11].

A basic shape of CTAH generated as in Fig. 3 where AQBY is lower reflector, DP′X is upper reflector, P′Q is aperture and XY is the absorber surface.

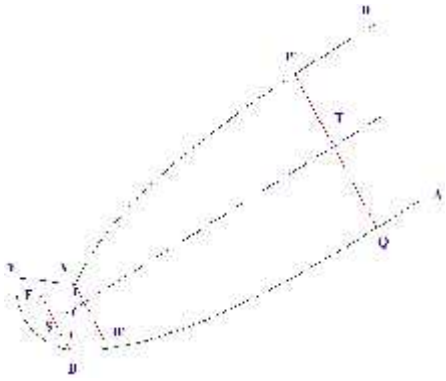

Fig. 3: Basic shape of CTAH

3. Design of the integrated concentrating air heating system

The optical concentrator is a part of the Concentrating Transpired Air-heating (CTAH) system as presented in Figure 4. This paper proposes an optical design of the concentrator. Four design improvements has been shown in Figure 3.

1) Inverted perforated absorber: A downward facing perforated absorber has been incorporated in the design which reduce radiation loss. Perforated surface allows air to flow through the absorber which enhances heat transfer between the absorber and flowing air.

Instead of a heavy metal absorber, a nonconventional low conductive light weight carbon fibre absorber has been used for the first time as the absorber material of the proposed collector. A fan is placed at the end of the air duct to extract air through the perforated absorber. The concentrator of the system works as an amplifier which increases the amount of solar radiation on a decreased absorber area.

2) Concentrator: A concentrator has been introduced with the perforated absorber for the first time to increase the concentration of the incident solar radiation onto the inverted perforated absorber. ACPC in CTAH has been designed with upper and lower reflectors of identical reflectance. Upper reflector is a combination of primary parabolic and straight tertiary reflector.

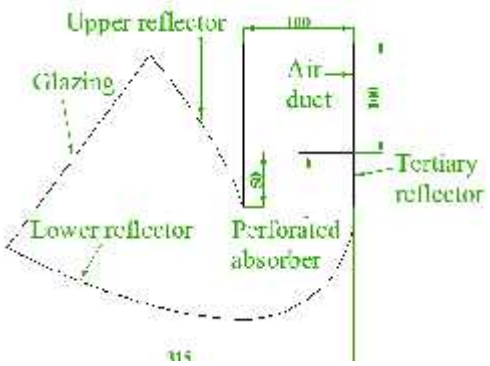

Fig. 4: Schematic diagram of the CTAH

Lower reflector is a combination of parabolic primary, circular secondary and straight tertiary reflectors. The secondary circular part of the concentrator in CTAH concentrates all incident radiation on the inverted absorber. The concentration ratio between inlet and outlet of the secondary circular reflector is 1. Concentration of solar radiation becomes necessary when higher temperatures are desired. Heat losses from the collector are proportional to the absorber area. Concentration ratio is the ratio of aperture area to absorber area. So, heat losses are inversely proportional to the concentration.

3) Tertiary reflector section: A parallel reflector section just below the inverted absorber helps to improve the stratified thermal layer below the absorber which enhances the heat transfer mechanism.

4) Glazing cover: A glazing cover has been introduced which works as the heat trap for the emitted radiation from the absorber surface. However, an optical loss occurs due to the reflection and absorption on the glazing cover. A high transmittance glazing material reduces the optical loss. Also during outdoor operation a glazing surface is necessary to provide protection from dust deposition, rain and wind. In conventional solar collectors a parallel glazing cover usually orients with absorber surface to reduce the reflection loss. However the design introduces convection loss from the glazing cover and radiation loss from the absorber surface. In the proposed design the absorber is placed at downward facing orientation.

4. Ray tracing modelling assumptions

The following modelling assumptions were made when developing the 2D ray trace model:

- all reflectors were considered to be specular, i.e. the angle of incidence equals the angle of reflection. The incident ray, the reflected ray and the normal at the point of intersection are considered to be in the same plane;
- the incident direct solar flux at the aperture was assumed to be a number of parallel rays each carrying equal amounts of energy;
- the reflectivity of all reflectors was 95%;
- the absorber was a perfect blackbody for the purpose of absorption;

- positive real values of x and y coordinates used to model the concentrator surfaces and rays;
- the CTAH aperture was tilted at an angle equal to the latitude of the location;
- the transmittance of the glazing was assumed to be 88%.

5. Solution of individual ray intersect concentrator surface

5.1 Calculation for the lower parabolic reflector

The co-ordinates of source points and the incident angles are known inputs of the simulation. For a particular angle of incidence, rays intersect the reflector surface. In the simulation model the value of the coordinates of the intersection points are always greater than zero, because all the calculations are on the positive axis.

To calculate the average number of reflections, all reflection paths of the incident rays were traced. Radiation passes through the aperture surface inclined at 53.3^o. The incident radiation equation is a function of the incident angle and point on the glazing cover.

As a result, the law of reflection on an intersection point on the parabola is applicable only considering each point exists in a different plane. The change in plane has to be considered in the calculation. As it can be seen, the ray intersects the lower parabola and reflects towards the circular reflector. It then reaches the absorber after another reflection on the circular reflector.

Figure 5 illustrates the calculation process of a single ray incident on the lower parabolic reflector from the aperture. The calculation process was repeated for 120,000 numbers of rays during the optical calculation of the concentrator. However for representation 120 rays are shown in upper section of the Figure 5.

Figure 6 presents the corresponding calculation of incident angles, reflection angles and intersection point. For a radiation source point A, the ray AB intersects the lower parabola at intersection point B. The values of angles at the intersection point B on the lower parabolic surface become: Slope of angle of the polynomial corresponding to the positive x-axis = CBC'.

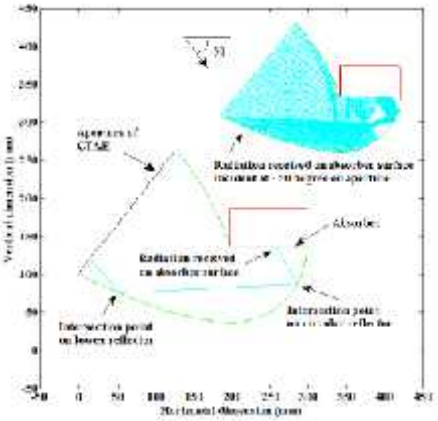

Fig. 5: Ray incident at -50^{o}incident angle on lower parabolic reflector

Assuming specular reflection, the rays follow the law of reflection on a highly reflective surface of the reflector. So, the incident angle ABB' = Reflection angle B'BE. The incident ray AB reflects on the lower reflector B at an angle CBE from the positive x axis and intersects the circular surface at point E. The centre of the circular reflector is at O. The ray BE reflects on the circular reflector surface at an angle BED and intersects the absorber as DE. The angle can be calculated from the positive x axis of point B as shown in the Figure 6. The necessary angles were calculated in Matlab at each point of intersection for all incident rays. However, the calculations are complicated for all rays incident on the lower parabola using Matlab for particular angles of incidence.

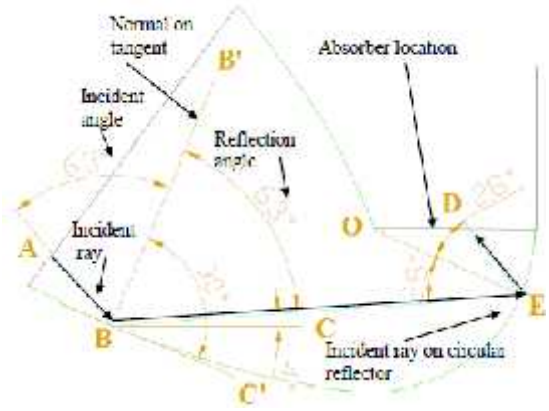

Fig. 6: Important angles to find the absorbed radiation for rays incident at -50^{o}incident angle on the lower parabolic reflector

Because the angle CBE changes direction from positive to negative as the y co-ordinate of the reflection rays at the incident point of lower parabola becomes negative. Similar phenomenon occurs on the circular reflector surface in case of multiple reflections inside the circular reflector surface. These changes are considered in this simulation model.

5.2 Calculation for the upper parabolic reflector

To calculate the average number of reflections, all reflection paths of the incident rays were traced after reflection from the upper reflector. The rays may intersect on the lower parabola or the circular reflector or may miss the lower reflector.

The upper reflector is more active for rays entering aperture at low incident angles with the vertical during summer days at solar noon. Figure 7 shows details of the calculation process of a single ray incident on the upper parabolic reflector from the aperture and the corresponding calculation of incident angles, reflection angles and intersection points. The calculation process for the upper reflector is more complicated. The calculation process was repeated for 120,000 rays during the optical calculation of the concentrator. For a radiation source point A, the ray AB intersects the upper parabola at intersection point B. In a similar way as detailed above, it can be shown that Incident angle ABC = Reflection angle CBD.

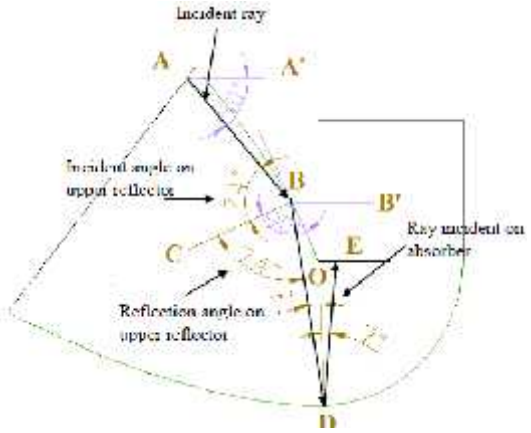

Fig. 7: Incident and reflection angles for incident ray on the upper reflector surface

The incident ray AB reflects on the upper reflector B at an angle negative B′BD from the positive x axis and intersects the lower reflector surface at point D and intersects the absorber at DE. The angle can be calculated from the positive x axis of point B as shown in Figure 7 for the upper reflector and point D of the lower reflector.

The formulas were used in Matlab to calculate the necessary angles on each point of intersection for all incident rays. However, the calculation of all rays incident on the lower reflector surface from the upper parabola is complicated using Matlab. Because for particular angles of incidence, the reflection angle B′BD can be less than 90^o or greater than 90^o. In both cases the result is completely different. Again when the reflection rays from the upper parabola intersect the lower reflector, it may intersect the parabolic part or the circular part. The exact intersection points have to be calculated independently in the simulation.

5.3 Calculation for the circular reflector

Figure 8 illustrates the calculation process for a ray incident directly on the circular reflector from the aperture. The rays reach the circular reflector directly only at higher incident angle from the vertical. The surface also concentrates rays after reflection from the upper and lower parabolic reflector. To calculate the average number of reflections, all reflection paths of incident rays were traced after reflection from the circular reflector.

The visualisation of an incident ray intersecting the circular reflector from the aperture has been shown in Figures 8. The incident radiation reaches the invertedabsorber after one reflection on the circular reflector surface. For a radiation source at point A shown in Figure 8, the ray AB intersects the circular reflector at intersection point B. In a similar way as detailed above, it can be shown that Incident angle ABO = Reflection angle CBO.

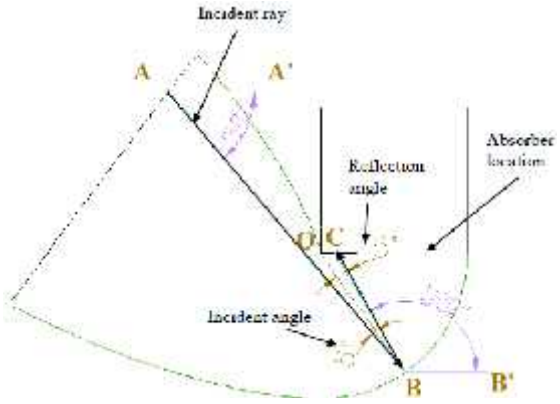

Fig. 8: Incident and reflection angles for incident rays directly on the circular reflector

The centre of the circular reflector section is O. The circular section basically concentrates all the incident radiation on the inverted absorber at a concentration ratio 1 until a ray intersects the centre before it reaches the circular reflector section. In that case, ray reflects back toward aperture.

The formulas are used in Matlab to calculate the necessary angles on each point of intersection for all incident rays on the circular reflector. However, if the reflection angle B′BC becomes less than $90^o$from the positive x axis, the ray experiences multiple reflections inside the circle. A case of multiple reflections has been shown in Figure 9 in the laser test of the model.

6. Ray tracing model validation

Laser visualisation tests were setup during the optical design process to provide a validation of both the Matlab model and its limits of operation as in Figure 9.

A physical model for the laser test is shown in the Figure 9(a). This is basically a cross section of the prototype made with 95% reflective alanod reflector used in the prototype. The frame of the setup was made of wood. A laser source was used as the light source. Five tests were carried out to test the reflector surfaces.

Fig. 9: (a) Ray-trace analysis setup

Test 1 is shown in Figure 9 (b), a laser ray intersecting the upper parabolic reflector and the reflected ray intersects the circular reflector. The ray reaches the inverted absorber

surface after reflection from the circular reflector. Test 2 is shown in Figure 9 (c). It explains how a laser ray intersects the circular surface directly from the aperture of the system.

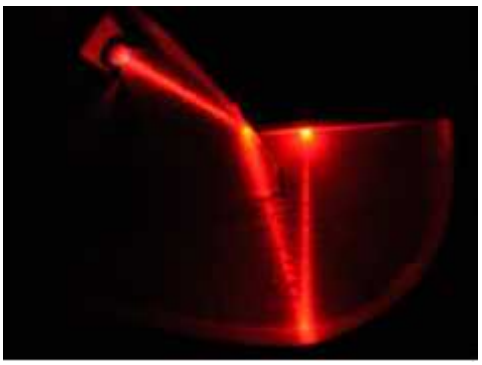

Fig. 9: (b) Test-1 Laser ray on upper reflector of CTAH

Fig. 9: (c) Test-2 Laser ray on circular reflector of CTAH

Fig. 9: (d) Test-3, Laser on lower parabola of CTAH

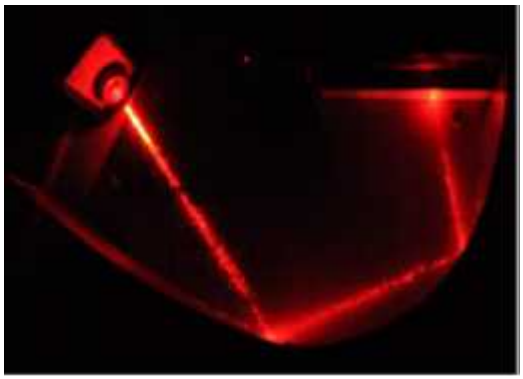

Fig. 9: (e) Test-4, Laser (Two reflections) on lower parabolic reflector of CTAH

Fig. 9: (f) Test-5, Laser (Three reflections) on lower parabola and circular reflector of CTAH

The ray reflects from the circular reflector and intersects the absorber surface. The circumstance is explained in Figures 6 to 8.Tests 3, 4 and 5 are illustrated in Figures 9 (d)-(f) respectively.Rays intersect the parabolic reflector at different points with different angle of incidence reaching the absorber after one or more than one reflections.Results of tests 1, 2, 3, 4 and 5 are presented in Figures 9 (b)-(f) demonstrate good affiliation to the ray-tracing results and these provided the confidence to build the prototype of the system.

7. Simulation results and analysis

The ray tracing model of the CTAH provides vital information about the system performance which includes:

a) average number of incident rays reflected before it reaches the absorber for each particular incidence angle;

b) instantaneous optical efficiency of the incident rays that reach the absorber;

c) visualisation of the incident rays, intersection points on the reflector boundary line and on the absorber surface; and

d) intensity of received ray distribution on the absorber surface for every individual incident angle.

The optical efficiency was calculated using the ray tracing model. The calculated optical efficiency was used as an input parameter in the heat transfer simulation model of the CTAH which was used to predict thermal performance of CTAH. The detailed thermal model with experimental validation will be discussed in future publication.

7.1 Optical performance of CTAH concentrator

Both diffuse and beam components of the incoming solar radiation are considered to calculate total available solar radiation on the aperture of the CTAH system. Rays incident on the CTAH from different directions are reflected by the reflector surface.

The imperfections in a real concentrator surface [3, 10] give optical errors that combine with a real radiation source to yield an effective radiation source [3]. The effective source Seff(θ) is the angular distribution that describes how much radiation is incident from the direction θ on the aperture of a

perfect reflector. The radiation intercepted by the receiver is defined by the angular acceptance functions $f(\theta)$ as the function of a uniform beam of parallel rays incident on the aperture at an angle θ that would reach the receiver if the optics were perfect [1-3].

Therefore, the intensity of radiation on the aperture from the direction θ reaching the absorber becomes Seff(θ)$f(\theta)$. The optical efficiency of the CTAH is defined as the fraction of solar radiation incident on the aperture which reaches and is absorbed by the absorber [11].

$$\eta_{Optical} = \frac{S}{I_{global}}$$

S = total energy absorbed (diffuse and direct)

Iglobal= total energy incident on the aperture (diffuse and direct)

The angular acceptance was determined as shown in Figure 10. All the incident rays on the concentrator surface from the aperture have more than one reflection before intersecting the inverted absorber.The reflectors are not identical asymmetric structures. It can be seen from the Figure 10 that the angular acceptance functions are not symmetric for all acceptance angles.

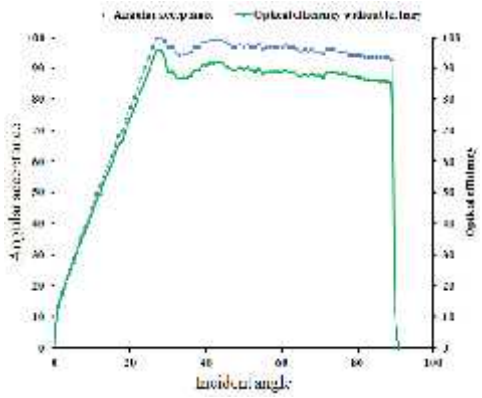

Fig. 10: The angular acceptance and optical efficiency for the CTAH without tertiary section

The angular acceptance and the optical efficiency for the CTAH have been shown without the tertiary section and with 95% reflector reflectance.

7.2 Effect of number of rays on optical performance

Individual rays undergo different numbers of reflections inside the concentrator surface before it reaches the absorber surface. Each number of reflections on the concentrator surface indicates a portion of optical loss from the available solar radiation. However, the optical loss inside the cavity increases the thermal energy of air in the cavity. The geometrical construction of the CTAH is a complex shape of different surfaces.

A deterministic approach to ray tracing was adopted that considered specular incident rays where every intersection point and reflection angles inside the concentrator cavity was calculated. The error reduces as the used number of rays increased.However, an enlarged number of rays increased the simulation time significantly. An analysis was carried out to find an optimum number of rays to reduce calculation errors. An increase in the number of rays from 125 to 12,500 reduced the percentage error to approximately 1.1% as shown in Figure 11.

The error reduced to 0.19% when the number of rays increased from 12,500 to 125,000 as can be seen from the coincidence of the curves for 12,500 rays and 125,000 rays in Figure 11. The results presented in this chapter are calculated for 125,000 rays to minimise the percentage error. It can be seen that the efficiency varies with incident angle. The highest efficiency was observed above 90% within acceptance angle.

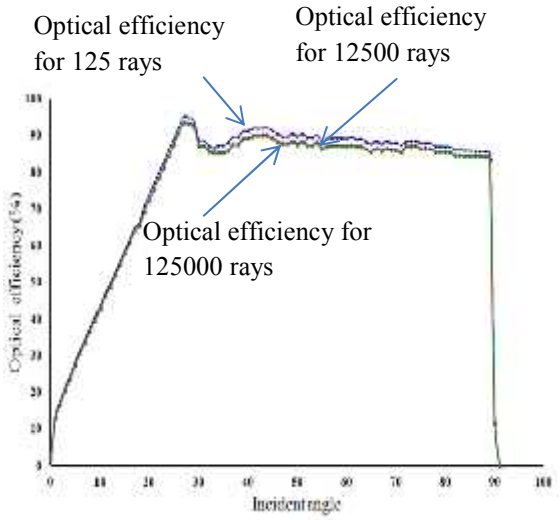

Fig. 11: Optical efficiency of the CTAH without the tertiary section for different number of rays (125 rays, 12,500 rays and 125,000 rays)

7.3 Effect of tertiary section and reflector reflectivity on optical performance

Figure 12 illustrates the intensity (rays/mm) of concentrated rays on the inverted absorber without the tertiary height.

As can be seen in Figure 12, peaks occur near the outer end of the absorber. It can also be seen that the concentrated insolation incidence is non-uniform over the absorber surface. The tertiary section and the reflectivity of the reflector are two factors which affect the optical efficiency of the CTAH over different incident angles. Another factor is the distribution of concentrated radiation over the absorber surface.

Figure 13 presents the intensity (rays/mm) of concentrated rays on the CTAH absorber with 50mm tertiary height. As can be seen in Figure 13, peaks shift towards the middle of the absorber's width. Again, it can be seen that the concentrated insolation incidence is non-uniform over the absorber width. The increase in tertiary height allows the radiation to increase uniformly over the absorber width which is desirable for improved system performance.

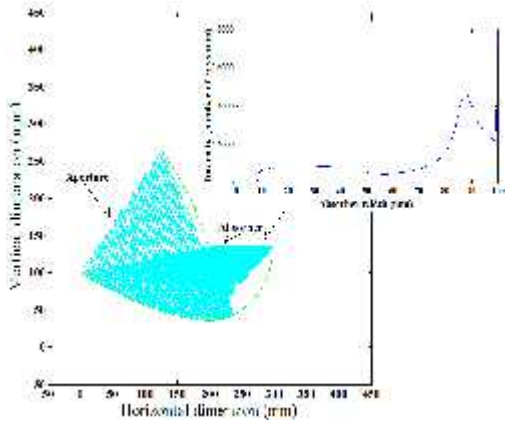

Fig. 12: Concentration of incident rays at 27° incident angle and 0 mm tertiary height

The tertiary reflector is supposed to be highly reflective to avoid increasing reflection loss due to higher number of reflections within the tertiary section.

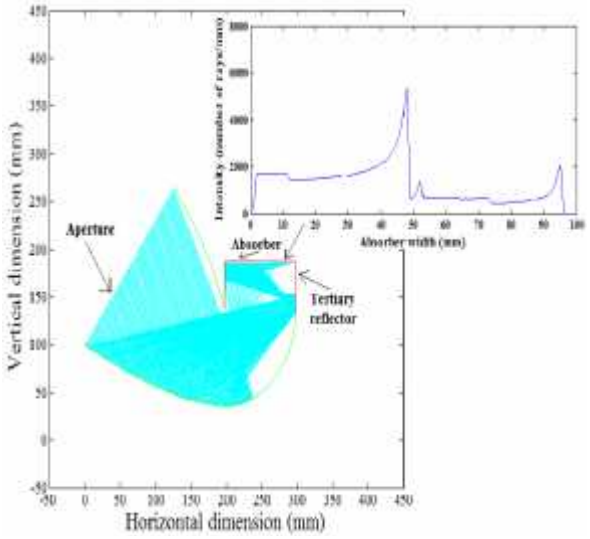

Fig. 13: Concentration of incident rays at 27° incident angle and 50 mm tertiary height

However, optical losses withinthe cavity and tertiary section increase the thermal energy of air in the cavity. Figure 14 details the intensity (rays/mm) of concentrated rays with 100mm tertiary height. As can be seen in Figure 14, peaks are more distributed over the absorber width. However, the concentrated insolation is non-uniform.

Figure 15 shows the effect of tertiary height from 0 mm to 100 mm and reflector reflectivity from 90% to 95% on optical efficiency of the concentrator.The concentrator efficiency is the maximum at zero tertiary height. The highest level of the optical efficiency was found for the reflector with 95% reflectivity. The lowest level of the optical efficiency was found for the reflector reflectivity of 90% and the tertiary height of 100 mm. It can be seen the optical efficiency increases with decreasing tertiary height and increasing reflector reflectivity.

However, it is a complex factor to define the higher significant factor between reflector reflectivity and tertiary height for optical efficiency of the CTAH. These analyses were carried out assuming the transmittance of the aperture is 100% to avoid the influence of transmittance on the results. Again improved reflector reflectivity (95%) enhanced optical efficiency. Considering 90% reflectivity of the concentrator surface, the 50 mm tertiary height reduced average optical efficiency by 5.4% and 100 mm tertiary reduced it by 10.2%.

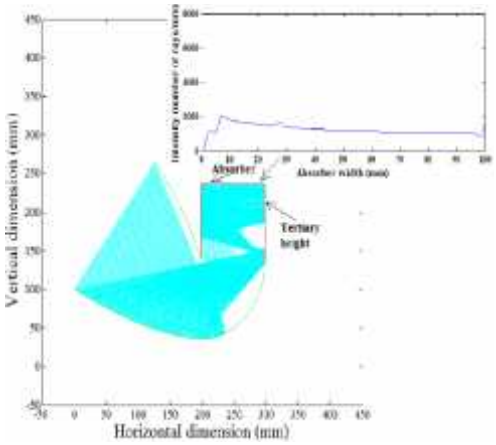

Fig. 14: Concentration of incident rays at 27°incident angle and 100 mm tertiary height for 125,000 rays

In case of a more reflective (95%) surface, the optical efficiency reduced by 2.7% for 50mm tertiary height and only 5.2% for 100 mm tertiary reflector cavity. This indicates that the effect of tertiary height is comparatively much lower for higher reflective surfaces.

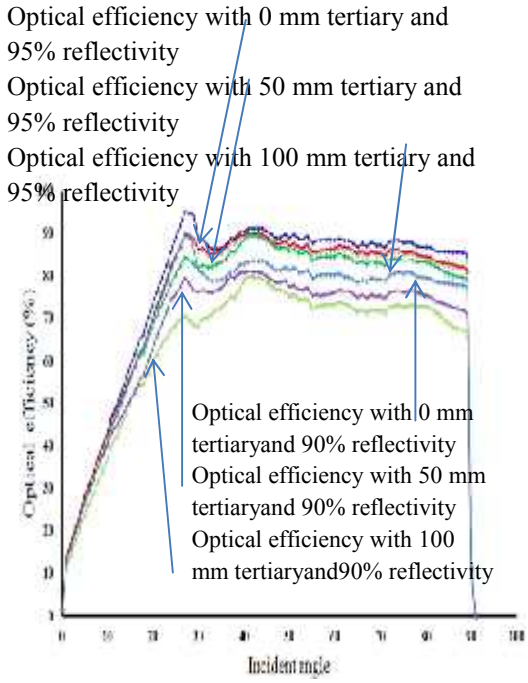

Fig. 15: Effect of tertiary height from 0 mm to 100 mm and reflector reflectivity from 90% to 95% on optical efficiency

A tertiary height is necessary to develop thermally stratified layer below absorber surface. Though the lowest tertiary height provides the highest optical efficiency, a straight tertiary height is necessary. To keep the optical efficiency loss due to combine effect of reflectivity and tertiary height at its minimum permissible range of 2.7% to 5.2%, the tertiary height needs to be maximum 50 mm and reflector reflectivity within 90-95%.

8. Conclusions

The basic optimisation factors considered in designing the CTAH system were to enhance the optical efficiency of the collector using a low concentration ratio concentrator; minimise the radiation and convection heat loss from absorber to ambient which can be achieved by using an inverted absorber facing downward; maximise convection heat transfer from absorber to inward airflow by using a perforated absorber and tertiary section to maintain a stable thermal layer in the concentrator cavity; minimise weight of the heating system by using a low weight perforated absorber; and minimise cost of the system by using unconventional low cost absorber material to avoid expensive selective coated metal absorber.

The maximum optical efficiency of the CTAH was 79.5% for 50 mm tertiary height, 88% transmittance of the glazing and 95% reflectance of the concentrator reflector for beam radiation. The acceptance angle of the CTAH varied between 100% at 27^o incident angle and 92.7% at incident angle 89^o which provides effective annual concentration for 7-8 hours. The optical efficiency within 27^o to 89^oincident angles varies between 79.5% and 72%.

The development of the ray tracing model using Matlab was described comprehensively. Boundary equations generation, calculation of intersection points and angles, ray tracing programming were detailed in developing the 2D ray tracing model of the CTAH. The validation process of the optical concentration was carried out using a laser test.The intensity of radiation on the absorber width was calculated using the model over different incident angles which were found to be non-uniform over the absorber width. The effect of tertiary height, reflector reflectivity and glazing cover on optical performance were analysed. The optical efficiency of the CTAH is used as an input of the heat transfer model. The optical design was used to construct prototypes of the CTAH system.

Reference

1. Rabl, A. (1985). *Active Solar Collectors and Their Applications*. New York: Oxford University Press.
2. Rabl, A. (1976). Comparison of solar concentrators. *Solar Energy, 18*(2), 93-111.
3. Welford, W. T., & Winston, R. (1978). *The Optics of Non-imaging Concentrators: Light and Solar Energy*. New York: Academic Press.
4. Winston, R. (1974). Principles of solar concentrators of a novel design. *Solar Energy, 16*(2), 89-95.
5. Norton, B., Kothdiwala, A. F., & Eames, P. C. (1994). Effect of inclination on the performance of CPC solar energy collectors. *Renewable Energy, 5*(1–4), 357-367.
6. Kothdiwala, A. F., Eames, P. C., & Norton, B. (1996). Optical performance of an asymmetric inverted absorber compound parabolic concentrating solar collector. *Renewable Energy, 9*(1–4), 576-579.
7. Kothdiwala, A. F., Norton, B., & Eames, P. C. (1995). The effect of variation of angle of inclination on the performance of low-concentration-ratio compound parabolic concentrating solar collectors. *Solar Energy, 55*(4), 301-309.
8. Norton, B., Kothdiwala, A. F., & Eames, P. C. (1994). Effect of inclination on the performance of CPC solar energy collectors. *Renewable Energy, 5*(1–4), 357-367.
9. Eames, P. C., Norton, B., & Kothdiwala, A. F. (1996). The state of the art in modelling line-axis concentrating solar energy collectors. *Renewable Energy, 9*(1–4), 562-567.
10. Mallick, T. K. (2003). *Optics and heat transfer for asymmetric compound parabolic photovoltaic concentrators for building integrated photovoltaics.* (Ph.D), University of Ulster, Uk.
11. Duffie, J. A., & Beckman, W. A. (2006). *Solar Engineering of Thermal Process* (3rd ed.). NY: J. W. & Sons.